doi.org/10.1002/cbdv.202300269 Research Article CHEMISTRY & BIODIVERSITY

www.cb.wiley.com

Design, Synthesis and Cytotoxicity of New Coumarin-1,2,3-triazole Derivatives: Evaluation of Anticancer Activity and Molecular Docking Studies

Victor Premsagar Miriyala,[a] Prakash Raj Thommandru,[a] Jajula Kashanna,*[b] Varadhi Govinda,[c] Guguloth Ravi,[d] and Ravada Kishore*[a]

A library of new coumarin-1,2,3-triazole hybrids **7a–l** were synthesized from 4-(diethylamino)-2-hydroxybenzaldehyde precursor through a series of reactions including Vilsmeier-Haack reaction and condensation reaction to achieve key intermediate oxime and further performed click reaction by using different aromatic azides. We screened all molecules in silico against crystal structure of Serine/threonine-protein kinase 24 (MST3), based on these results all molecules were screened for their cytotoxicity against human breast cancer MCF-7 and lung cancer A-549 cell lines. Compound **7b** (*p*-bromo) showed best activity against both cell lines MCF-7 and A-549 with IC_{50} value of 29.32 and 21.03 μM, respectively, in comparison to *Doxorubicin* corresponding IC_{50} value of 28.76 and 20.82 μM. Another compound **7f** (o-methoxy) also indicated good activity against both cell lines with IC_{50} value of 29.26 and 22.41 μM. The toxicity of all compounds tested against normal HEK-293 cell lines have not shown any adverse effects.

1. Introduction

Over the last few decades, the incidences of lethal diseases have grown more rapidly throughout the globe, and their effects are also increased daily and lead to death. In this context, there is a need to develop effective new drugs to prevent those fatal diseases such as cancer,[1,2] viral attacks,[3–5] etc. Moreover, one of the most irremediable diseases is cancer; it significantly impacts humanity and leads to death. Cancer deaths account for millions of deaths per year worldwide.[6,7] However, chemotherapy is one of the best treatment methods for reducing the growth and stopping cancer cells compared to other available treatment methods such as stem cell transplantation, radiation therapy and immune therapy.[8] Moreover, scientists around the globe have struggled and a way found to cure or prevent cancer. As a result, only a few inhibitory small molecules are coming into the market, and many are in clinical trials only. Even now, there are no effective drugs available for cancer treatment. Drugs from medicinal plants have an advantage over synthetic drugs due to their availability, and no side effects towards enhancing the quality of health of cancer patients. Few research groups discovered drugs like coumarin and their derivatives from plant materials effectively reduced incurable diseases in humans.[9,10]

The coumarin molecules are familiar and notorious moities with several applications, and vital action is occurring in arrears to concession of shape and physicochemical properties of the 2-benzopyrone entity.[11–14] However, coumarin and its derivatives were found to have a wide range of biological and pharmaceutical activities and have been used as good activity agents over decades for the cure of cancer and HIV,[15] coagulant,[16] oxidant[17] and inflammatory[18] and also used as the fascinating aspects to control or to heal of asthma and arthritis.[19] The synthesized derivatives of coumarin and D-galactose moieties reports of Toan and coauthors showed worthy of action against EGFR–L858R and EGFR–T790 M tyrosine kinase.[13] Thus, these compounds act as significant agents for metabolic agents and are used as aromas in the manufacturing of food materials in the industry such as food additives, cosmetics and perfume ingredients. Thus, the coumarin and its derivatives have glaringly played a significant and extensive role in the arena of anti-tumor therapy from last few years.[20] Mostly, the more active epidermal growth factor receptor (EGFR) can play a vital role in the growth and development of certain belligerent types of breast cancer.[12,13] Indeed, coumarin derivatives are found as essential drug agents for treating metabolic diseases. Furthermore, 4-hydroxycoumarin was used to reduce the reverse transcriptase activity of ACH-2-lymphocyte affected by the HIV[21] and the acylation of hydroxy groups at C-7&C-8 positions of 7,8-dihydroxycoumarin and C-7 position of the 7-hydroxycoumarin skeleton were elucidated the changing of G-protein-coupled receptor activators into inhibitors.[22,23] Moreover, 3*E*-3-(4-methylbenzylidene)-

[a] *V. Premsagar Miriyala, P. Raj Thommandru, Dr. R. Kishore*
Department of Chemistry, School of Science, GITAM (Deemed to be University), Visakhapatnam-530045, India
E-mail: kravada@gitam.edu

[b] *Dr. J. Kashanna*
Department of Chemistry, Rajiv Gandhi University of Knowledge Technologies-Basar, Nirmal-504107, India
E-mail: jajulakashanna@rgukt.ac.in

[c] *Dr. V. Govinda*
Department of Chemistry, Gayatri Vidya Parishad College, Visakhapatnam-530045, India

[d] *Dr. G. Ravi*
Department of Chemistry, University College of Science, Osmania University, Hyderabad, Telangana-500007, India

Supporting information for this article is available on the WWW under https://doi.org/10.1002/cbdv.202300269

3,4-dihydro-2H-chromen-2-one and Warfarin derivative were found to an excellent anticancer agent to MCF-7 and HT-29 cells with diverse concentrations exhibited considerable cytotoxicity for breast cancer peoples[24] and 7-(carboxymethoxy)-4-methyl coumarin was prescribed to patients who suffered with upper or lower limb i.e., lymphedema disease.[25] Due to heterocyclic conformational discrepancy in the coumarin derivatives of 1,2,3-Triazole, these compounds project fascinating aspects to have specific binding with tumor cells and to control the growth of cancer cells in mitochondria and human serum albumin.[26,28]

Molecular docking is a computational procedure that aims to predict the favored orientation of a ligand to its macromolecular target (receptor) when these are bound to each other to form a stable complex.[29] It is a reliable, cost-effective, and time-saving technique in the process of drug discovery.[30] Molecular docking is a rapidly growing platform in Computer Aided Drug Discovery and Design (CADDD).[31] Autodock Vina integrated PyRx is an open-source virtual screening tool most widely used for in silco studies.[32–36]

However, additional attempts are still required to improve the remedial use of these drugs to complete healing of breast cancer. Moreover, Feng Gao and co-authors have elucidated that 1,2,3-triazole-containing compounds were working as good anti-lung cancer agents and clearly explained their mechanism in the treatment of lung cancer development as a novel anti-lung cancer agent with new technology with low toxicity and high efficacy.[26] Therefore, in continuation of our work[27] on the construction of bioactive products, we have designed different coumarin-1,2,3-triazole derivatives to check whether they are special stabilizers and may fetch some changes in the breast cancer cells' anatomy. In this study, coumarin-1,2,3-triazole derivatives are synthesized and designed from 4-(diethylamino)-2-hydroxybenzaldehyde through a series of reactions including Vilsmeier-Haack reaction (formylation step), condensation followed by click reaction.

However, we have studied the binding of synthesized coumarin derivatives with breast cancer cells under physiological conditions with phosphate buffer (pH 7.4). In the present study, we have depicted the influence of coumarin derivatives on cytotoxic activity against four cancer cell lines. Besides, to understand the knowledge of structural activity relationship, it studies the cancer cells by performing the experimental and molecular docking analysis. For Molecular docking studies we selected Mst3 In complex with Cdk1/2 Inhibitor III, 5-Amino-3-{[4-(Aminosulfonyl)Phenyl]Amino}-N-(2,6-Difluorophenyl)-1h-1,2,4-Triazole-1-Carbothioamide (PDB_ID 4QMP). These MST (Mammalian Sterile20-like) kinases emerged as key signaling molecules that influenced cell proliferation, cell migration, organ size, and cell polarity. Recent studies reported that malfunctions in those MST kinases may result in cancer, endothelial malformations, and a few autoimmune diseases. MST3 is a member of the STRIPAK complex, the deregulation of which has recently been associated with cancer cell migration and metastasis. Targeting MST3 with small-molecule inhibitors may be beneficial for the treatment of certain cancers, but little information exists on the potential of kinase inhibitor scaffolds to engage with MST3. Hence, we have chosen this protein complex and accordingly we designed our synthesized compounds to develop as a novel small molecule inhibitor.[37,38] Increasing and focused studies have suggested the key roles of MST mammalian Sterile20-like (MST) family of kinases in many aspects of biology. Molecular docking studies explains the relationship between the active binding sites of coumarin-1,2,3-triazole based derivatives and targeted proteins.

Theoretical results of coumarin-1,2,3-triazole derivatives afford to predict different binding sites through molecular modeling and also support the coumarin substitution which is more active in the entire protein molecule. Eventually, the molecular docking results have maintained various efficacies against cytotoxic associated with breast cancer cells (MCF-7) and lung cancer (A549) cells. The structure and stability of the cancer cells in the presence of coumarin-1,2,3-triazole have received particular interest in biochemical, biological, and pharmaceutical adaptation. To the best of our attention, there is no more literature on the structure and stability of breast cancer cells with the effect of coumarin-1,2,3-triazole derivatives. Consequently, this study may help to determine the aspects in the literature which cannot be avoided from the requirement for future researchers who will work on tumor cells with the effect of coumarin-1,2,3-triazole and its derivatives.

2. Results and Discussion

2.1. Chemistry

Synthetic route of (*E*)-7-(diethylamino)-2-oxo-2*H*-chromene-3-carbaldehyde O-((substituted-phenyl-1*H*-1,2,3-triazol-4-yl)methyl) oxime (**7a–l**) were represented in Scheme 1. Derivatives of the coumarin-1,2,3-triazoles (**7a–l**) were carried out by cyclisation of 4-(diethylamino)-2-hydroxybenzaldehyde (**1**) using DMF in PPA at room temperature for 2–3 h to afford 7-(diethylamino)-2*H*-chromen-2-one (**2**) followed by Vilsmeier-Haack reaction in presence of DMF and $POCl_3$ to afford 7-(diethylamino)-2-oxo-2*H*-chromene-3-carbaldehyde (**3**). Which on further conversion of oxime in presence of hydroxylic amine hydrochloride methanol and sodium acetate for 1 hr (at room temperature) to afford (*E*)-7-(diethylamino)-2-oxo-2*H*-chromene-3-carbaldehyde oxime(**4**), in constitution compound **4** was treated with propargyl bromide yields to (*E*)-7-(diethylamino)-2-oxo-2*H*-chromene-3-carbaldehyde O-prop-2-yn-1-yl oxime (**5**). Which on further click reaction of substituted aryl azides (**6a–l**) at the terminal alkyne position (**5**) in presence of sodium ascorbate and copper salt to afford the compounds with 1,2,3-triazole tethered 7-(diethylamino)-2-oxo-2*H*-chromene hybrids (**7a–l**). The products were obtained in good yields (75–82%). All the newly synthesized coumarin-1,2,3-triazole derivatives (**7a–l**) were characterized by FT-IR, MS, ^{1}H-NMR and ^{13}C-NMR. In FT-IR spectra, compound 7b showed stretching absorption bands at 1518 cm^{-1}, 1221 cm^{-1}, and 2969 cm^{-1} for N=N, C–N of triazole moiety, and C–H bonds, respectively. The imine and lactone carbonyl functions showed stretching bands at 1617 cm^{-1} and 1703 cm^{-1}. The other compounds of series **7**(**a–l**) shows similar

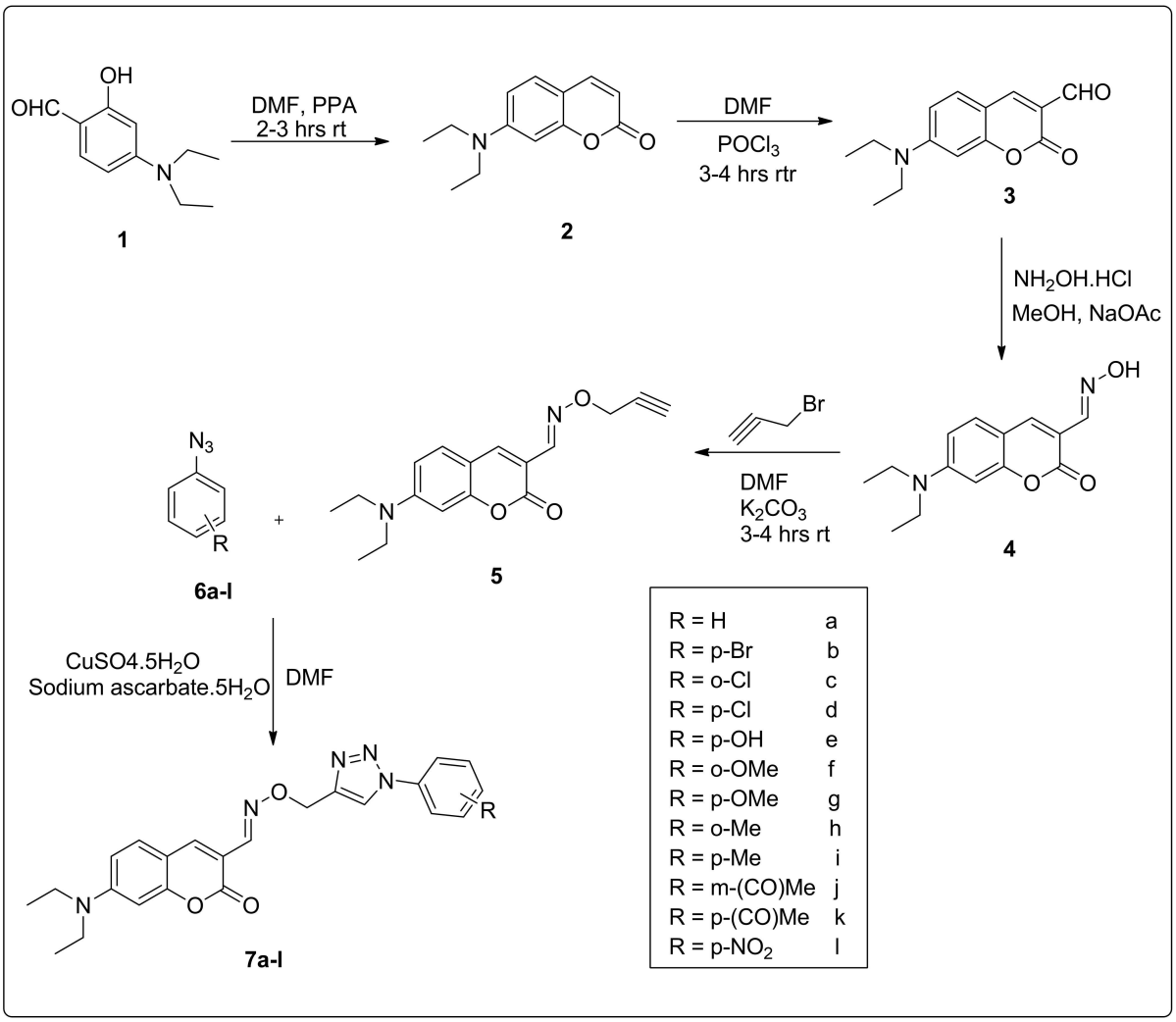

Scheme 1. Synthetic route representation of compounds **7a**–**7l**.

and consistent pattern absorption bands in their respective IR spectra. The ^{1}H-NMR spectrum of compound **7b** shows a triplet at δ 1.43 ppm for CH_3, **7c**, **7f**, **7i**, **7k** and **7l** show triplets at 1.18 ppm, and **7g** and **7h** shows triplets at 1.17 ppm, and **7a**, **7d**, **7e** and **7j** at δ 1.19, 1.14, 1.19 and 1.15 ppm, respectively. The compound **7a** and **7d** shows a quartet at δ 3.37 and 3.34, and **7b**, **7k**, **7l** at δ 3.46 whereas **7c** and **7f**–**j** at δ 3.50 ppm for N–CH_2 protons. The compounds **7a**, **7e** and **7l** shows a singlet at δ 4.71, 4.86 and 5.32 ppm for O–CH_2 protons, whereas **7b**, **7g** at δ 5.29, and **7c**, **7d**, **7f** and **7k** at δ 5.31 ppm. Further, **7b**, **7g** and **7j** shows a singlet at δ 5.29 ppm for O–CH_2 protons. The compounds **7a**–**l** showed the signals within the range δ 8.23–9.06 ppm for triazole ring, δ 6.56–7.86 ppm for imine protons and the signals within the range of δ 6.75–8.31 ppm for C_4-H protons. Further, all compounds showed a multiplet within the range of δ 6.84–8.23 ppm aromatic protons in their respective spectra. The compounds **7a**–**l** showed resonance signals within the range of δ 12.4–12.8, δ 41.2–54.9, and δ 62.6–63.9 ppm, respectively for N-ethyl CH_3, CH_2 and O–CH_2 carbons in their ^{13}C-NMR spectra. The aromatic OCH_3 carbon of **7f** and **7g** shows a resonance signal at δ 55.7 and 55.4 ppm, whereas **7h** and **7i** shows signal at δ 17.3 and 21.2 ppm. All compounds of series **7a**–**l** showed the signals in the range δ 139.8–153.81 ppm, δ 142.39–155.48 ppm and δ 162.9–197.2 ppm for C_4-, C10- and lactone-carbonyl carbons, respectively. The other signals appeared in the aromatic and substituent carbons absorption region. The synthesized compounds **7a**–**l** showed the base peaks corresponding to their molecular mass in their mass spectra. However, in addition to the base peaks, compounds **7b**, **7c** and **7d** showed a (M + 2) peak corresponds to ^{37}Cl and ^{81}Br isotopic masses.

2.2. Molecular Docking Studies

Serine/threonine-protein kinase 24 (MST3) promotes proliferation and tumorigenicity, its over expression is observed in breast as well as lung cancer cells.[39] As a reason we have chosen the crystal structure of MST3 (PDB ID: 4QMP) as in silico target. The novel coumarin – triazole hybrids were docked into

the cavity of crystal structure of MST3 using Autodock Vina integrated PyRx virtual screening tool,[32,40,41] and presented the docking scores and binding interactions in Table 1. The docking results were validated by re-docking the co-crystalized ligand 5-amino-3-{[4-(aminosulfonyl)phenyl]amino}-n-(2,6-difluorophenyl)-1h-1,2,4-triazole-1-carbothioamide (DKI), it produced an RMSD value of 1.025 Å and scored binding energy value of −8.8 kcal/mole.

The *p*-bromo substituted analog **7b** scored highest docking score of −9.1 kcal/mol, greater than the score of DKI. The **7b** demonstrated key interactions with MST3 at amino acid sites Ile30, Lys32 (two interactions) and Asp109 with bond distance of 3.27, 1.73, 2.65 and 3.15 Å, respectively, these interactions are important for formation of ligand – target complex. In addition, hydrophobic interactions were executed Ile30, Gly31, Val38, Ala51, Met99, Tyr101, Ser106, Ala148, Leu151, Ala161and Asp162 in cavity of MST3 (Figure 1). The second highest docking score of −9.0 was reported by *o*-methoxy substituted ligand **7f**. It was also indicated H-bond interactions with Ile30, Lys32 (two interactions) and Asp109, their bond distances were recorded as 3.17, 1.75, 2.61 and 3.13 Å, respectively, in cavity of MST3. Further, hydrophobic interactions were established with amino acid sites Ile30, Gly31, Val38, Ala51, Met99, Gly105, Ser106, Asp109, Ala148, Leu151, Ala161 and Asp162 of MST3 (Figure 2). The co-crystallized ligand DKI indicated H-bond interactions with Lys32, Met99, Asp109 and Asp162, hydrophobic interactions were shown with Ile30, Val38, Ala51, Lys53, Met99, Glu100, Ser106, Asp109, Ala148 and Leu151 of MST3 (Figure 3). Almost all the compounds exhibited H-bond interactions like DKI at active sites of MST3 (Lys32 or Asp109 or Asp162). The hydrophobic interactions of the compounds also matching with DKI interactions, which reveal that these compounds could best fit into the cavity of MST3.

Table 1. Docking scores and binding interactions of compound **7a–l** against Serine/threonine-protein kinase 24 (MST3).

Entry	Binding Energy	Interacting Amino acids	
		H-bonding interactions	Hydrophobic interactions
7a	−8.7	Lys32, Ser106, Ala148, Asn149	Ile30, Val38, Ala51, Met99, Tyr101, Leu151, Ala161, Asp162
7b	−9.1	Ile30, Lys32, Asp109	Ile30, Gly31, Val38, Ala51, Met99, Tyr101, Ser106, Ala148, Leu151, Ala161, Asp162
7c	−8.9	Ile30	Ile30, Val38, Ala51, Lys53, Met99, Tyr101, Gly104, Ser106, Asp109, Leu151, Ala161, Lys292
7d	−8.2	Ile30, Lys32	Ile30, Val38, Ala51, Met99, Asp109, Ala148, Leu151, Ala161, Asp162
7e	−8.7	Lys32, Ala148, Asn149	Ile30, Lys32, Val38, Ala51, Met99, Leu102, Ala148, Leu151, Ala161, Asp162,
7f	−9.0	Ile30, Lys32, Asp109	Ile30, Gly31, Val38, Ala51, Met99, Gly105, Ser106, Asp109, Ala148, Leu151, Ala161, Asp162
7g	−8.4	Asp162	Ile30, Val38, Ala51, Tyr101, Leu108, Asp109, Ala148, Leu151, Ala161
7h	−8.9	Asp162	Ile30, Val38, Ala51, Me99, Ala148, Leu151, Ala161
7i	−8.8	Lys32	Ile30, Val38, Ala51, Lys53, Met99, Tyr101, Leu102, Asp109, Ala148, Leu151, Ala161
7j	−8.9	Leu102, Ala148	Ile30, Val38, Met99, Asp109, Ala148, Leu151, Ala161
7k	−8.2	Ile30, Leu102, Asp109, Lys146	Ile30, Val38, Met99, Asp109, Ala148, Leu151, Ala161
7l	−8.8	Lys32, Leu102	Ile30, Val38, Lys53, Met99, Asp109, Ala148, Leu151, Ala161, Asp162
DKI	−8.8	Lys32, Met99, Asp109, Asp162	Ile30, Val38, Ala51, Lys53, Met99, Glu100, Ser106, Asp109, Ala148, Leu151

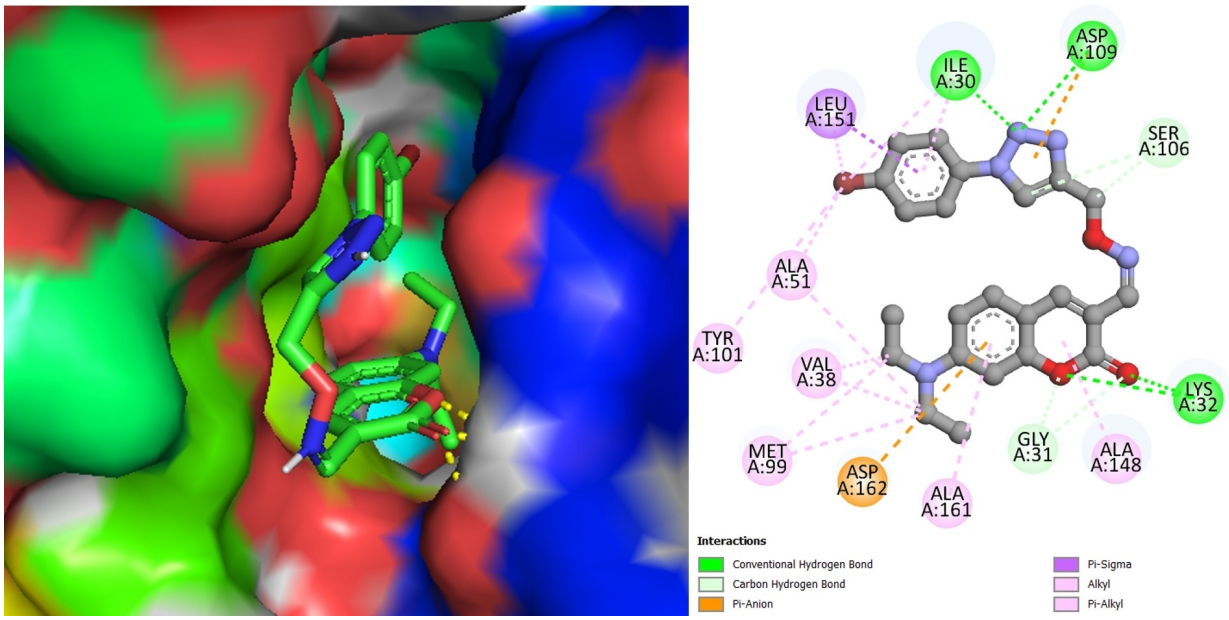

Figure 1. Docking pose and binding interactions of compound **7b** in cavity of MST3.

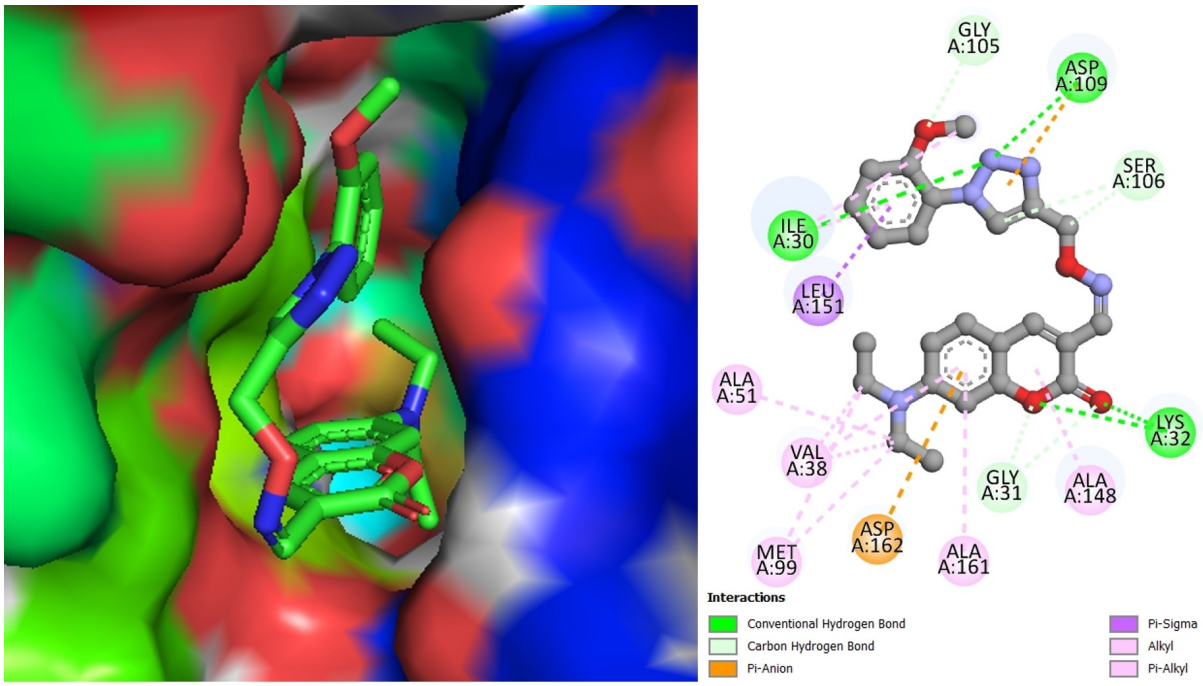

Figure 2. Docking pose and binding interactions of compound **7f** in cavity of MST3.

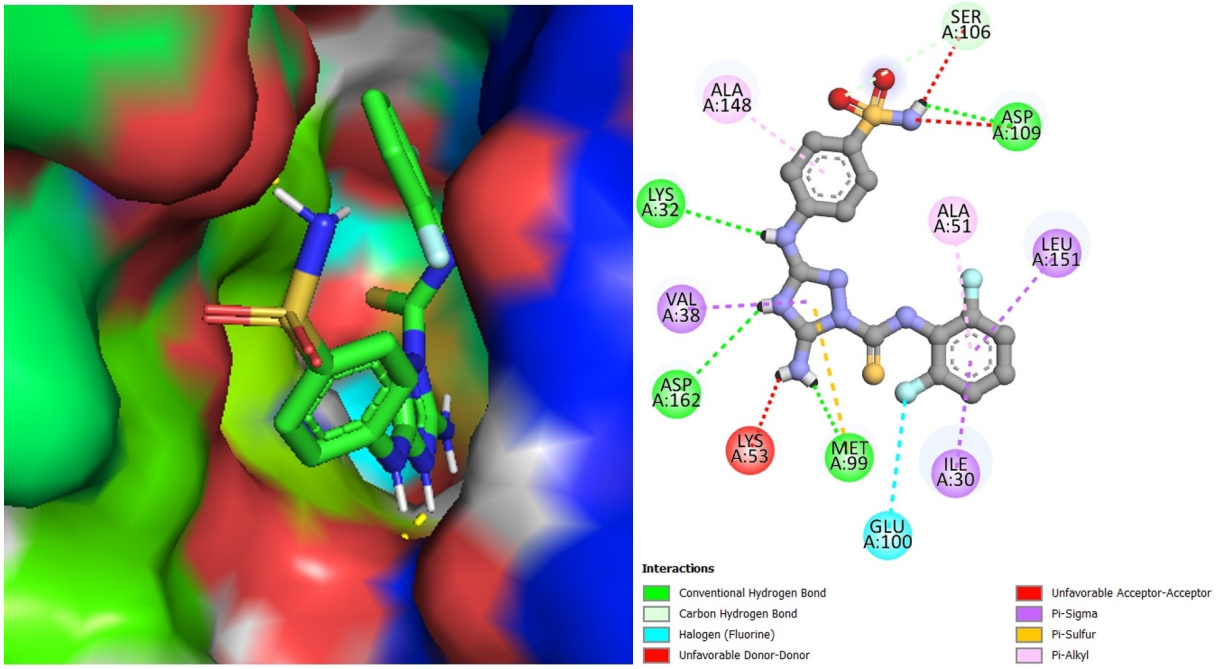

Figure 3. Docking pose and binding interactions of DKI in cavity of MST3.

2.3. Pharmacokinetics

The pharmacokinetic properties of all compounds 7a–l were predicted by using SwissADME web server[42] and are tabulated in Table 2. The octanol/water partition coefficient (Log Pw/o) values were anticipated in the range of 3.70–4.52, and as per the essential condition of Lipinski's rule of five.[43] The molecular weights of all compounds are $\leq$500 g/mol, they can be easily transported, absorbed, and diffused after administered into the body.[44] The predicted rotatable bonds were in the range of 8–9, H-bond acceptors were $\leq$10, and H-bond donors were absent. The topological polar surface (TSPA) of analogous were in the range of 85.75–131.75; these lower TSPA values indicate the acceptable range of results. The violations of Lipinski's rule

Table 2. Pharmacokinetic properties of compounds **7a—l**.

Compound	Molecular weight (range ≤ 500)	Rotatable bonds (range 1–10)	H-bond acceptors (range ≤ 10)	H-bond donors (range ≤ 5)	TPSA	Log $P_{o/w}$ (range ≤ 5)	Molar refractivity (Range 40–130)	QPLogS (Solubility)	Lipinski violations	Bioavailability Score (range 0.4–0.6)	Synthetic Accessibility
7a	417.46	8	6	0	85.75	3.87	120.25	−4.91	0	0.55	3.91
7b	496.36	8	6	0	85.75	4.52	127.95	−5.82	0	0.55	3.92
7c	451.91	8	6	0	85.75	4.09	125.26	−5.50	0	0.55	3.89
d	451.91	8	6	0	85.75	4.37	125.26	−5.50	0	0.55	3.91
7e	433.46	8	7	1	105.98	3.70	122.27	−4.77	0	0.55	3.94
7f	447.49	9	7	0	94.98	4.22	126.74	−4.98	0	0.55	4.01
7g	447.49	9	7	0	94.98	4.31	126.74	−4.98	0	0.55	4.00
7h	431.49	8	6	0	85.75	4.07	125.22	−5.21	0	0.55	4.03
7i	431.49	8	6	0	85.75	3.80	125.22	−5.21	0	0.55	4.01
7j	459.50	9	7	0	102.82	3.82	130.45	−4.86	0	0.55	4.04
7k	459.50	9	7	0	102.82	4.07	130.45	−4.86	0	0.55	4.02
7l	462.46	9	8	0	131.57	3.72	110.55	−4.96	1	0.55	3.99

were zero. The synthetic accessibility score of all analogs was found to be <10, it confirms that they can be synthesized easily.[45] The pharmacokinetic evaluation reveal that all molecules have favourable drug-likeness properties and could be considered as therapeutic agents.

2.4. Cytotoxicity

Based on the docking result we have carried out invitro anticancer activity of all compounds against human breast cancer MCF-7 and human lung cancer A-549 cell lines. Tested their toxicity against normal embryo kidney cells (HEK293). The MTT assay was employed using *Doxorubicin* as standard reference at various concentration (600, 300, 150, 75, 37.5, 18.75 μg/mL) of test compounds were treated. The calculated IC_{50} value of compounds (**7a–l**) presented in Table 3. Interestingly, the *p*-bromo compound **7b** showed best activity against both cell lines MCF-7 and A-549 with IC_{50} value of **29.32** ± 1.28 and **21.03** ± 1.22 **μM**, respectively, in comparison to *Doxorubicin* corresponding IC_{50} value of **28.76** ± 1.18 and **20.82** ± 1.16 **μM**. Compounds **7f** and **7l** executed good activity against MCF-7 cell lines with IC_{50} value of **29.26** ± 1.08 and **29.62** ± 1.09 **μM**, respectively. Also, compounds **7d**, **7h** and **7l** indicated good activity against the A-549 cell lines with IC_{50} value of **24.92** ± 1.61, **24.88** ± 2.12 and **23.08** ± 1.08 **μM**, respectively. Whereas the remaining compounds exhibited moderate to poor activity. The toxicity of the compounds tested against normal HEK-239 cell lines have not shown any adverse effect. The activity of these compounds may be attributed to the presence of electron withdrawing functions such as Cl, OH, OMe, NO_2 and COOMe which makes the molecule electron deficient in turn it binds to the electron rich site of target protein. Also, the presence of triazole and phenyl rings enable the π–π stacking and π-T shaped interactions. Further, the N and O atoms present in moiety could act as H-bond acceptors.

3. Conclusions

Eventually from our reports clearly observed the potential role of anti-cancer drugs of the coumarin-1,2,3-triazole derivatives

Table 3. IC_{50} value of compounds **7a–l** against MCF-7 and A-549 cell lines.

Compound	MCF-7	A-549	HEK293
7a	52.82% ± 1.42	49.06% ± 1.67	110% ± 1.07
7b	29.32% ± 1.28	21.03% ± 1.22	98% ± 1.34
7c	38.82% ± 1.86	36.36% ± 1.75	103% ± 1.22
7d	31.02% ± 1.64	24.92% ± 1.61	120% ± 1.06
7e	33.41% ± 1.37	32.89% ± 1.57	110% ± 1.14
7f	29.26% ± 1.08	22.41% ± 1.24	97% ± 1.26
7g	34.12% ± 1.20	26.06% ± 1.12	104% ± 1.08
7h	32.62% ± 1.03	24.88% ± 2.12	106% ± 1.52
7i	53.28% ± 1.09	47.03% ± 1.92	160% ± 1.26
7j	34.31% ± 1.12	31.10% ± 1.01	110% ± 1.41
7k	51.82% ± 1.45	46.06% ± 1.87	123% ± 1.36
7l	29.62% ± 1.29	23.08% ± 1.08	97% ± 1.18
Doxorubicin	28.76% ± 1.18	20.82 ± 1.16	97% ± 1.22

7a–l are play an vital role in the stabilization of protein. The breast cancer cells and lung cancer cells have shown enhanced activity, stability and selectivity in the presence of the **7b** and **7f** coumarin derivatives when compared to reference compound Doxorubicin. Therefore, the compounds **7b** and **7f** can be identified as potent anti-cancer activity agents for controlling the growth of cancer cell in the human beings. In continuation, among all the title compounds, compounds **7b** and **7f** (highest docking score compounds); **7c, 7h** & **7j** (equal score compounds) exerted significant anti-cancer properties against select cancer cell lines. Overall, *in vitro* anti-cancer studies in combination with the in silico molecular docking studies exemplifies the significance of rational design and development of hybrid hetero structures containing active pharmacophores.

Experimental Section

General experimental methods

Purchased all the chemical material of the organic reagents and solvents from TCI, Merck Chemical Company, were used without further purification. The materials are maximum grade level for synthesis of organic compounds. Compounds **2**–**6** are prepared as per the literature procedures.[46–53]

Instrumentation

^{1}H-NMR and ^{13}C-NMR spectra were determined in DMSO by using 500 and 125 MHz spectrometers (Instrument Bruker Avance II 500 MHz). Chemical shift values are displayed as ppm and spin multiplicities are indicated as singlet (s); doublet (d); doublet of doublet (dd); triplet (t); multiplets (m); and coupling constants are shown in hertz. Column chromatography was performed on silica gel (60–120 mesh) using distilled hexane and ethyl acetate solvents. Micro analytical (C, H, N) data were obtained with a FLASH EA 1112 Series CHNS Analyzer. Mass and Infrared spectra were recorded on Bruker ALPHA II, ECO-ATR. Melting points were determined in open glass capillary tube on a DbkProg. Melting Point apparatus and were uncorrected.

General procedure for the preparation of (E)-7-(diethylamino)-2-oxo-2H-chromene-3-carbaldehyde oxime (4)

The synthetic route for the (*E*)-7-(diethylamino)-2-oxo-2*H*-chromene-3-carbaldehyde oxime (4) was carried out by taking 7-(diethylamino)-2-oxo-2*H*-chromene-3-carbaldehyde (**3**) as starting material and it is converted to oxime in presence of hydroxylic amine hydrochloride methanol and sodium acetate at room temperature for 1 h.

General procedure for the preparation of (E)-7-(diethylamino)-2-oxo-2H-chromene-3-carbaldehyde O-prop-2-yn-1-yl oxime (5)

The synthetic route for the (*E*)-7-(diethylamino)-2-oxo-2*H*-chromene-3-carbaldehyde O-prop-2-yn-1-yl oxime (**5**) was carried out by refluxing the prepared oxime compound (**4**) as starting material and propergylic bromide in dry DMF and dry K_2CO_3 at room temperature for 3–4 h proporgylation takes place at the position of free O–H group on oxime to yield (E)-7-(diethylamino)-2-oxo-2*H*-chromene-3-carbaldehyde O-prop-2-yn-1-yl oxime (**5**). The product formation was monitored by using TLC.

General procedure for the preparation of (E)-7-(diethylamino)-2-oxo-2H-chromene-3-carbaldehyde O-((substituted-phenyl-1H-1,2,3-triazol-4-yl) methyl) oxime (7a–l)

Synthesis of (*E*)-7-(diethylamino)-2-oxo-2*H*-chromene-3-carbaldehyde O-((substituted-phenyl-1*H*-1,2,3-triazol-4-yl) methyl) oxime (**7a**–**l**) were carried out by using click chemistry reaction of propargylated compound (**5**) (0.1 mmol) with different aryl azides (**6a**–**l**) (0.1 mmol) in $CuSO_4.5H_2O$ with sodium ascorbate and DMF at room temperature for 6–8 hr. The completion of the reaction was monitored by TLC. Upon completion of the reaction, pure compound was isolated by column chromatography using hexane/ethyl acetate (1 : 3 v/v) with excellent yields 75–82 %.

Anticancer activity

Maintenance of cell lines:

Breast cancer and lung cancer cell lines MCF-7, A549 were purchased from the National Center for Cell sciences (NCCS) Pune. The cell lines were cultured in DMEM medium, i.e., Dulbecco's modified Eagle medium, which were supplemented with 10 % heat inactivated fetal calf serum (FBS) and 1 % Antibiotic-Antimycotic 100X solution and incubated in CO_2 incubator (Eppendorf Brunswick, Galaxy 170R, Germany) maintained at 37 °C, 5 % CO_2 with 95 % humidity until the completion of experiments.

MTT Assay

The breast cancer cell lines and lung cancer cells (A549 &MCF-7) and normal embryo kidney cells (HEK293) cultured in DMEM medium, which was supplemented with 10 % heat inactivated fetal calf serum (FBS) and 1 % Antibiotic-Antimycotic 100X solution. The cells were seeded at a density of approximately 5×10^3 cells/well in a 96-well flat-bottom micro plate and maintained at 37 °C in 95 % humidity and 5 % CO_2 for overnight. Different concentration (600, 300, 150, 75, 37.5, 18.75 µg/mL) of test compounds were treated. The cells were incubated for another 72 h. The cells in well were washed twice with phosphate buffer solution, and 20 µL of the MTT staining solution (5 mg/mL in phosphate buffer solution) was added to each well and plate was incubated at 37 °C. After 4 h, 100 µL of dimethyl sulfoxide (DMSO) was added to each well to dissolve the formazan crystals, and absorbance was recorded with a 570 nm using micro plate reader. The IC_{50} values were calculated using graph Pad Prism Version5.1 (Table 2).

Molecular Docking studies

Autodock Vina integrated PyRx tool was employed for docking simulations.[54–56] The crystal structure of Serine/threonine-protein kinase 24 (MST3) (PDB ID: 4QMP)[57] were retrieved from Protein Data Bank (www.rcsb.org). Initially, water molecules and heteroatoms of protein were removed and added polar hydrogens. The ligands were sketched using ChemDraw Professional 16.0 in MDL file format. Minimized the energies of all ligands after loading into PyRx and converted to PDBQT file format. The 3D grid box was configured with dimensions of center_x = 26.11139776, center_y = −0.934122545682, center_z = 70.6270669435, size_x =

16.3716365317, size_y = 20.9680392342 and size z = 23.6855628891, docking simulations were performed after assigning the exhaustiveness value of 8. The docking results were visualized using Pymol and Biovia Discovery Studio Visualizer.

Spectral data

(*E*)-7-(diethylamino)-2-oxo-2*H*-chromene-3-carbaldehyde O-((1-phenyl-1*H*-1,2,3-triazol-4-yl)methyl) oxime (7a): Yield 80%, m.p.: 163–165 °C; Rf = 0.36 (AcOEt:hexane 2:3); IR (V_{max}, cm^{-1}): 2927, 1696, 1618, 1514, 1218, 1069. ^{1}H-NMR (500 MHz, (D_6)DMSO) δ 8.52 (s, 1H), 7.91 (s, 1H), 7.83 (d, *J* = 7.57, 2H), 7.69 (d, *J* = 8.43, 1H), 7.40 (dd, *J* = 7.57, 7.20, 4H), 7.09 (s, 1H), 6.84 (d, *J* = 8.43, 1H), 4.71 (s, 2H), 3.37 (q, *J* = 7.22, 4H), 1.19 (t, *J* = 7.22, 6.92, 6H). ^{13}C-NMR (125 MHz, (D_6)DMSO) δ 163.8, 156.2, 143.8, 138.5, 137.6, 135.2, 129.1, 127.3, 124.6, 124.1, 120.7, 116.4, 115.1, 110.7, 63.6, 44.5, 12.8. LC/MS *m/z*: 418.4 $[M+H]^+$ Elemental analysis, Calculated,%: $C_{23}H_{23}N_5O_3$:C, 66.17; H, 5.55; N, 16.78; Found%:C, 66.14; H, 5.50; N, 16.72.

(*E*)-7-(diethylamino)-2-oxo-2*H*-chromene-3-carbaldehyde O-((1-(4-bromophenyl)-1*H*-1,2,3-triazol-4-yl)methyl) oxime (7b): Yield 85%, m.p.: 160–162 °C; Rf = 0.43 (AcOEt:hexane 2:3); IR (V_{max}, cm^{-1}): 2969, 1703, 1611, 1518, 1221, 1061. ^{1}H-NMR (500 MHz, (D_6)DMSO) δ 8.95 (s, 1H), 8.23 (d, *J* = 7.60, 2H), 8.11 (d, *J* = 7.60, 4H), 6.75 (d, *J* = 8.43, 2H),6.84 (d, *J* = 8.43, 1H), 5.29 (s, 2H), 3.46 (q, *J* = 7.22, 4H), 1.4 (t, *J* = 7.22, 6.92, 6H). ^{13}C-NMR (125 MHz, (D_6)DMSO) δ 164.6, 152.9, 151.5, 150.3, 142.8, 141.8, 133.7, 133.6, 128.7, 120.9, 119.9, 119.8, 113.2, 109.2, 99.0, 63.7, 44.2, 12.4. LC/MS *m/z*: 497.3 $[M+H]^+$ Elemental analysis, Calculated,%:$C_{23}H_{22}BrN_5O_3$: C, 55.66; H, 4.47; N, 14.11; Found%:C, 55.62; H, 4.42; N, 14.07.

(*E*)-7-(diethylamino)-2-oxo-2*H*-chromene-3-carbaldehyde O-((1-(2-chlorophenyl)-*1H*-1,2,3-triazol-4-yl)methyl) oxime (7c): Yield 79%, m.p.: 161–163 °C; Rf = 0.43 (AcOEt:hexane 2:3); IR (V_{max}, cm^{-1}): 2976, 1695, 1611, 1520, 1228, 1061. ^{1}H-NMR (500 MHz, (D_6)DMSO) δ 8.56 (s, 1H), 8.23 (s, 1H), 7.86 (s, 1H), 7.72 (d, *J* = 7.52, 2H), 7.42 (dd, *J* = 7.57, 7.49, 3H), 6.87 (s, 1H), 6.80 (dd, *J* = 7.51, 7.50, 1H), 5.31 (s, 2H), 3.50 (q, *J* = 7.22, 4H), 1.18 (t, *J* = 7.22, 6.92, 6H).^{13}C-NMR (125 MHz, (D_6)DMSO) δ 164.6, 152.9, 151.5, 142.8, 141.6, 134.4, 130.5, 128.7, 128.5, 128.0, 121.1, 119.8, 119.3, 111.3, 109.2, 98.9, 63.9, 44.2, 12.4. LC/MS *m/z*: 452.2$[M+H]^+$ Elemental analysis, Calculated,%:$C_{23}H_{22}ClN_5O_3$:C, 61.13; H, 4.91; N, 15.50; Found%:C, 61.09; H, 4.87; N, 15.45.

(*E*)-7-(diethylamino)-2-oxo-2*H*-chromene-3-carbaldehyde O-((1-(4-chlorophenyl)-1*H*-1,2,3-triazol-4-yl)methyl) oxime (7d): Yield 82%, m.p.: 164–166 °C; Rf = 0.41 (AcOEt:hexane 2:3); IR (V_{max}, cm^{-1}): 2976, 1695, 1611, 1520, 1229, 1061. ^{1}H-NMR (500 MHz, (D_6)DMSO) δ 8.94 (s, 1H), 8.23 (d, *J* = 7.52, 2H), 7.96 (d, *J* = 7.51, 2H), 7.61 (d, *J* = 7.52, 3H), 6.75 (s, 1H), 6.56 (s, 1H), 5.31 (s, 2H), 3.34 (q, *J* = 7.22, 4H), 1.14(t, *J* = 7.22, 6.92, 6H).^{13}C-NMR (125 MHz, (D_6)DMSO) δ 164.6, 152.9, 151.5, 150.2, 142.8, 141.6, 133.1, 132.9, 129.9, 128.7, 121.5, 119.9, 119.8, 111.3, 109.2, 98.9, 63.6, 44.2, 12.4. LC/MS *m/z*: 452.2$[M+H]^+$ Elemental analysis, Calculated,%: $C_{23}H_{22}ClN_5O_3$:C, 61.13; H, 4.91; N, 15.50; Found%:C, 61.09; H, 4.87; N, 15.45.

(*E*)-7-(diethylamino)-2-oxo-2*H*-chromene-3-carbaldehyde O-((1-(4-hydroxyphenyl)-1*H*-1,2,3-triazol-4-yl)methyl) oxime (7e): Yield 75%, m.p.: 156–158 °C; Rf = 0.32 (AcOEt:hexane 2:3); IR (V_{max}, cm^{-1}): 3320, 2973, 1695, 1611, 1520, 1229, 1061. ^{1}H-NMR (500 MHz, (D_6)DMSO) δ 9.58 (s, 1H), 8.52 (s, 1H), 7.94 (s, 1H), 7.63 (d, *J* = 8.43, 1H), 7.59 (d, *J* = 8.43, 2H), 7.38 (s, 1H), 7.09 (s, 1H), 6.85 (d, *J* = 8.43, 2H), 6.84 (d, *J* = 8.43, 1H), 4.86 (s, 2H), 3.37 (q, *J* = 7.22, 4H), 1.19 (t, *J* = 7.22, 6.92, 6H). ^{13}C-NMR (125 MHz, (D_6)DMSO) δ 163.8, 157.3, 156.0, 143.8, 138.5, 137.6, 135.2, 126.8, 124.6, 124.3, 120.7, 116.4, 115.2, 115.1, 110.1, 63.6, 54.9, 12.8. LC/MS *m/z*: 434.3 $[M+H]^+$ Elemental analysis, Calculated,%:$C_{23}H_{23}N_5O_4$: C, 63.73; H, 5.35; N, 16.16; Found%:C, 63.69; H, 5.28; N, 16.12.

(*E*)-7-(diethylamino)-2-oxo-2*H*-chromene-3-carbaldehyde O-((1-(2-methoxyphenyl)-1*H*-1,2,3-triazol-4-yl)methyl) oxime (7f): Yield 82%, m.p.: 143–145 °C; Rf = 0.40 (AcOEt:hexane 2:3); IR (V_{max}, cm^{-1}): 2971, 1699, 1600, 1516, 1247, 1029. ^{1}H-NMR (500 MHz, (D_6)DMSO) δ 8.50 (s, 1H), 8.23 (s, 1H), 7.86 (s, 1H), 7.72 (d, *J* = 7.50, 2H), 7.25 (dd, *J* = 7.49, 7.51, 2H), 7.02 (d, *J* = 7.49, 1H), 6.87 (s, 1H), 6.80 (d, *J* = 7.53, 1H), 5.31 (s, 2H), 3.80 (s, 3H), 3.50 (q, *J* = 7.22, 4H), 1.18 (t, *J* = 7.22, 6.92, 6H).^{13}C-NMR (125 MHz, (D_6)DMSO) δ 164.7, 154.0, 152.9, 151.9, 150.2, 142.8, 128.7, 128.1, 127.5, 123.4, 121.9, 119.8, 118.4, 114.7, 111.3, 109.2, 98.9, 98.9, 63.9, 55.7, 44.2, 12.4. LC/MS *m/z*: 448.3 $[M+H]^+$ Elemental analysis, Calculated,%: $C_{24}H_{25}N_5O_4$:C, 64.42; H, 5.63; N, 15.65; Found%:C, 64.38; H, 5.59; N, 15.62.

(*E*)-7-(diethylamino)-2-oxo-2*H*-chromene-3-carbaldehyde O-((1-(4-methoxyphenyl)-1*H*-1,2,3-triazol-4-yl)methyl) oxime (7g): Yield 84%, m.p.: 144–146 °C; Rf = 0.42 (AcOEt:hexane 2:3); IR (V_{max}, cm^{-1}): 2968, 1699, 1600, 1516, 1247, 1029. ^{1}H-NMR (500 MHz, (D_6)DMSO) δ 8.62 (s, 1H), 8.23 (s, 1H), 7.86 (s, 1H), 7.72 (d, *J* = 7.50, 1H), 7.62 (d, *J* = 7.50, 2H), 7.09 (d, *J* = 7.51, 2H), 6.87 (s, 1H), 6.80 (d, *J* = 7.49, 1H), 5.29 (s, 2H), 3.81 (s, 3H), 3.50 (q, J = 7.22, 4H) 1.17 (t, *J* = 7.22, 6.92, 6H).^{13}C-NMR (125 MHz, (D_6)DMSO) δ 164.7, 158.4, 152.9, 151.5, 150.2, 142.8, 141.6, 129.0, 128.7, 120.9, 119.9, 119.8, 116.3, 111.3, 109.2, 98.9, 63.6, 55.4, 44.2, 12.4. LC/MS *m/z*: 448.2 [M + H]+ Elemental analysis, Calculated,%:$C_{24}H_{25}N_5O_4$:C, 64.42; H, 5.63; N, 15.65; Found%:C, 64.38; H, 5.59; N, 15.62.

(*E*)-7-(diethylamino)-2-oxo-2*H*-chromene-3-carbaldehyde O-((1-(o–tolyl)-1H-1,2,3-triazol-4-yl)methyl) oxime (7h): Yield 78%, m.p.: 142–144 °C; Rf = 0.42 (AcOEt:hexane 2:3); IR (V_{max}, cm^{-1}): 2969, 1693, 1604, 1516, 1247, 1030. ^{1}H-NMR (500 MHz, (D_6)DMSO) δ 8.57 (s, 1H), 8.23 (s, 1H), 7.86 (s, 1H), 7.72 (d, *J* = 7.51, 1H), 7.64 (d, *J* = 7.49, 1H), 7.35 (dd, *J* = 7.52, 7.49, 3H), 6.87 (s, 1H), 6.80 (d, *J* = 7.49, 1H), 5.28 (s, 2H), 3.50 (q, *J* = 7.22, 4H), 2.27 (s, 3H), 1.17 (t, *J* = 7.22, 6.92, 6H).^{13}C-NMR (125 MHz, (D_6)DMSO) δ 164.6, 152.9, 151.5, 149.7, 142.8, 142.2, 135.4, 130.3, 130.2, 128.8, 127.5, 127.3, 120.3, 119.8, 118.4, 113.3, 109.2, 98.9, 63.9, 44.2, 17.3, 12.4. LC/MS *m/z*: 432.2$[M+H]^+$ Elemental analysis, Calculated,%:$C_{24}H_{25}N_5O_3$:C, 66.81; H, 5.84; N, 16.25; Found%:C, 66.78; H, 5.81; N, 16.21.

(*E*)-7-(diethylamino)-2-oxo-2*H*-chromene-3-carbaldehyde O-((1-(*p*–tolyl)-1*H*-1,2,3-triazol-4-yl)methyl) oxime (7i): Yield 80%, m.p.: 140–1138 °C; Rf = 0.41 (AcOEt:hexane 2:3); IR (V_{max}, cm^{-1}): 2973, 1701, 1600, 1517, 1249, 1025. ^{1}H-NMR (500 MHz, (D_6)DMSO) δ 8.62 (s, 1H), 8.23 (s, 1H), 7.86 (s, 1H), 7.72 (d, *J* = 7.51, 1H), 7.57 (d, *J* = 7.49, 2H), 7.33 (d, *J* = 7.50, 2H), 6.87 (s, 1H), 6.80 (d, *J* = 7.51, 1H), 5.28 (s, 2H), 3.50 (q, *J* = 7.22, 4H), 2.36 (s, 3H), 1.18 (t, *J* = 7.21, 6.90, 6H).^{13}C-NMR (125 MHz, (D_6)DMSO) δ 164.6, 152.9, 151.5, 149.7, 142.8, 141.6, 137.7, 132.7, 130.1, 128.8, 119.9, 119.8, 119.2, 111.3, 109.2, 98.9, 63.6, 44.2, 21.2, 12.4. LC/MS *m/z*: 432.2 $[M+H]^+$ Elemental analysis, Calculated,%:$C_{24}H_{25}N_5O_3$:C, 66.81; H, 5.84; N, 16.25; Found%:C, 66.78; H, 5.81; N, 16.21.

(*E*)-7-(diethylamino)-2-oxo-2*H*-chromene-3-carbaldehyde O-((1-(3-acetylphenyl)-1*H*-1,2,3-triazol-4-yl)methyl) oxime (7j): Yield 82%, m.p.: 161–163 °C; Rf = 0.40 (AcOEt:hexane 2:3); IR (V_{max}, cm^{-1}): 2971, 1700, 1604, 1516, 1251, 1020. ^{1}H-NMR (500 MHz, (D_6)DMSO) δ 8.56 (s, 1H), 8.31 (s, 1H), 8.23 (s, 1H), 7.88 (d, *J* = 7.49, 2H), 7.76 (d, *J* = 7.51, 2H), 7.60 (dd, *J* = 7.51, 7.50, 1H), 6.87 (s, 1H), 6.81 (d, *J* = 7.51, 1H), 5.29 (s, 2H), 3.50 (q, *J* = 7.22, 4H), 2.56 (s, 3H), 1.15(t, *J* = 7.20, 6.91, 6H). ^{13}C-NMR (125 MHz, (D_6)DMSO) δ 197.2, 165.0, 152.9, 151.5, 150.2, 142.9, 141.7, 136.3, 135.1, 129.7, 128.6, 127.3, 121.7, 120.7, 119.8, 118.0, 111.3, 109.2, 38.9, 63.6, 44.2, 26.7, 12.4. LC/MS *m/z*: 460.3 $[M+H]^+$ Elemental analysis, Calculated,%:

$C_{25}H_{25}N_5O_4$:C, 65.35; H, 5.48; N, 15.24; Found%:C, 65.30; H, 5.44; N, 15.19.

(*E*)-7-(diethylamino)-2-oxo-2*H*-chromene-3-carbaldehyde O-((1-(4-acetylphenyl)-1*H*-1,2,3-triazol-4-yl)methyl) oxime (**7k**): Yield 85%, m.p.: 165–167 °C; Rf = 0.40 (AcOEt:hexane 2:3); IR (V_{max}, cm^{-1}): 2973, 1704, 1604, 1521, 1251, 1038. ^{1}H-NMR (500 MHz, (D_6)DMSO) δ 9.06 (s, 1H), 8.26 (s, 1H), 8.18 (s, 2H), 8.08 (s, 3H), 7.61 (s, 1H), 6.78 (s, 1H), 6.56 (s, 1H), 5.31 (s, 2H), 3.46 (q, *J* = 7.22, 4H), 2.61 (s, 3H), 1.18(t, *J* = 7.22, 6.92, 6H). ^{13}C-NMR (125 MHz, (D_6)DMSO) δ 196.8, 165.0, 152.9, 151.5, 150.2, 142.9, 141.6, 137.8, 136.1, 130.0, 128.6, 119.9, 119.8, 118.6, 111.3, 109.2, 98.9, 63.6, 44.2, 26.4, 12.4. LC/MS *m/z*: 460.3 $[M+H]^+$ Elemental analysis, Calculated,%:$C_{25}H_{25}N_5O_4$:C, 65.35; H, 5.48; N, 15.24; Found%:C, 65.30; H, 5.44; N, 15.19.

(*E*)-7-(diethylamino)-2-oxo-2*H*-chromene-3-carbaldehyde O-((1-(4-nitrophenyl)-1*H*-1,2,3-triazol-4-yl)methyl) oxime (**7l**): Yield 82%, m.p.: 171–173 °C; Rf = 0.36 (AcOEt:hexane 2:3); IR (V_{max}, cm^{-1}): 2973, 1706, 1604, 1520, 1251, 1038. ^{1}H-NMR (500 MHz, (D_6)DMSO) δ 9.13 (s, 1H) 8.47 (d, *J* = 7.50, 2H), 8.27 (m, 3H), 8.12 (s, 1H), 7.56 (s, 1H), 6.76 (s, 1H), 6.56 (s, 1H), 5.32 (s, 2H), 3.46 (q, *J* = 7.22, 4H), 1.18(t, *J* = 7.22, 6.92, 6H). ^{13}C-NMR (125 MHz, (D_6)DMSO) δ 165.0, 152.9, 151.9, 150.2, 146.4, 142.9, 141.5, 139.9, 128.6, 126.0, 120.8, 119.9, 119.8, 111.3, 109.2, 98.9, 63.6, 44.2, 12.4. LC/MS *m/z*: 463.2 $[M+H]^+$ Elemental analysis, Calculated,%:$C_{23}H_{22}N_6O_5$:C, 59.73; H, 4.80; N, 18.17; Found%:C, 59.69; H, 4.75; N, 18.13.

Acknowledgements

RK acknowledges the DST-SERB for the financial support under the early career research award scheme (project no. ECR/2018/000637). We also thank University of Hyderabad and GITAM (Deemed to be University) for utilize the facilities.

Conflict of Interests

The authors declare no conflict of interest.

Data Availability Statement

The data that support the findings of this study are available in the supplementary material of this article.

Keywords: click reaction · coumarin derivatives · cytotoxicity · docking studies · Vilsmeier-Haack reaction

[1] O. Kazuki, I. Makoto, M. Kosuke, A. Takako, S. Akinori, *Cancer Sci.* **2020**, *111*, 112–126.
[2] J. E. Bolden, M. J. Peart, R. W. Johnstone, *Nat. Rev. Drug Discovery* **2006**, *5*, 769.
[3] L. Jiaye, L. Xuejiao, Q. Shen, Y. Jing, W. Fuxiang, L. Yingxia, W. Zhaoqin, W. Fu-Sheng, L. Lei, Z. Zheng, *Emerg. Infect Dis.* **2020**, *26*, 1320.
[4] D. Subrata, A. Scott, *Eur. J. Drug Metab. Pharmacokinetic* **2021**, *46*, 185–203.
[5] A. J. Rodriguez-Moralesabcde, J. A. Cardona-Ospina, E. Gutiérrez-Ocampo, R. Villamizar-Peña, Y. Holguin-Rivera, J. P. Escalera-Antezana, L. E. Alvarado-Arnez, D. K. Bonilla-Aldana, C. Franco-Paredes, A. F. Henao-Martinez, A. Paniz-Mondolfi, G. J. Lagos-Grisales, E. Ramírez-Vallejo, J. A. Suárez, L. I. Zambrano, W. E. Villamil-Gómez, G. J. Balbin-Ramon, A. A. Rabaan, S. Ranjit, *Travel Med Infect Dis.* **2020**, *34*, 101623.
[6] S. Bin, L. Serena, D. D. Danyetta, W. B. Robert, *J. Med. Chem.* **2007**, *50*, 1635–1644.
[7] J. C. Mathers, *Nutr. Res.* **2019**, *70*, 26–31.
[8] D. Sanjeev, K. Nagaraju, A. Paul, S. P. Ashona, T. S. Sourav, K. Mandeep, J. B. Sreekantha, S. Parvesh, *Bioorg. Med. Chem.* **2018**, *26*, 5612–5623.
[9] C. Samia, D. Meriem, R. Anne, D. Delphine, L. Olivier, B. J. Hichem, G. Rafik, *Bioorg. Chem.* **2018**, *80*, 189–194.
[10] T. Prakasam, M. Dariusz, J. Krzysztof, *Chem. Rev.* **2013**, *113*, 4905–4979.
[11] V. N. Toan, D. T. Nguyen, *New J. Chem.* **2021**, *45*, 10636–10653.
[12] D. T. Nguyen, S. H. Do, T. H. Le, T. H. Nguyen, M. H. Nguyen, T. N. B. Vu, T. T. H. Pham, N. T. Vu, T. K. V. Hoang, T. K. G. Nguyen, *New J. Chem.* **2022**, *46*, 23179–23197.
[13] V. N. Toan, D. T. Nguyen, *Med. Chem. Res.* **2021**, *30*, 1868–1885.
[14] Y. Wu, J. Xu, Y. Liu, Y. Zeng, G. Wu, *Front.Oncol.* **2020**, *10*, 592853.
[15] P. Thitima, S. Muney, H. H. Stephen, D. S. Djaja, M. P. John, *J. Nat. Prod.* **1996**, *59*, 839–842.
[16] J. P. Salvador, D. Tassies, J. C. Reverter, M. P. Marco, *Anal. Chim. Acta* **2018**, *1028*, 59–65.
[17] M. B. Bruno, B. Lorenzo, C. Eliana, C. Ignacio, C. Paola, T. P. Anna, N. Lucia, S. Raffaele, *J. Nat. Prod.* **2017**, *80*, 3247–3254.
[18] J. Lowenthal, H. Birnbaum, K. Vitamin, *Science* **1969**, *164*, 181–183.
[19] J. R. Hoult, R. A. Forder, B. de las Heras, I. B. Lobo, M. Paya, *Agents Actions* **1994**, *42*, 44–49.
[20] A. Carneiro, M. J. Matos, E. Uriarte, L. Santana, *Molecules* **2021**, *26*, 1–15.
[21] A. S. Bourinbaiar, R. Nagorny, *Acta Virol* **1993**, *37*, 21–28.
[22] F. Zhe, Z. Linjie, H. Sijin, W. Shiyi, L. Na, S. Xiaojing, W. Zian, S. Ruilong, W. Fang, W. Wenhui, G. Ruihua, *Polymer* **2022**, *14*, 1–13.
[23] Y. Wang, J. Wang, F. Zhe, S. Ruilong, W. Wenhui, J. Fan, R. G. Ruihua, *Bioorg. Chem.* **2020**, *104*, 104342–104351.
[24] T. Beena, L. Sudha, A. Nataraj, V. Balachandran, D. Kannan, M. N. Ponnuswamy, *Chem. Cent. J.* **2017**, *11*, 1–19.
[25] N. Farinola, N. Piller, *Lymphatic Res. Biol.* **2005**, *3*, 81–86.
[26] T. Liang, X. Sun, W. Li, G. Hou, F. Gao, *Front. Pharmacol.* **2021**, *12*, 1–20.
[27] J. Kashanna, R. A. Kumar, R. Kishore, D. Nandan Kumar, *Chem. Biodiversity* **2018**, *15*, e1800277.
[28] E. Ortega-Forte, A. Rovira, A. Gandioso, J. Bonelli, M. Bosch, J. Ruiz, V. Marchán, *J. Med. Chem.* **2021**, *64*, 17209–17220.
[29] T. Lengauer, M. Rarey, *Curr. Opin. Struct. Biol.* **1996**, *6*, 402–406.
[30] G. Yaku, D. Ramulu, V. Thumma, A. Paluri, R. Dharavath, *Chemistry Select* **2023**, *8*, e202300255.
[31] K. K. Chaudhary, N. Mishra, *JSM Chem.* **2016**, *4*, 1029.
[32] S. Dallakyan, A. J. Olson, *Meth. Mol. Bio.* **2015**, *1263*, 243–250.
[33] K. C. Veeranki, J. Pochampally, R. C. Maroju, V. Thumma, L. S. Boddu, *Asian J. Chem.* **2023**, *35*, 125–134.
[34] D. Veeranna, L. Ramdas, G. Ravi, S. Bujji, V. Thumma, J. Ramchander, *ChemistrySelect* **2022**, *7*, e202201758.
[35] A. K. Sabhavath, S. Madderla, R. Dharavath, V. Thumma, G. Thara, S. Gundu, A. Dongamanti, *ChemistrySelect* **2022**, *7*, e202203847.
[36] D. Ashok, G. Thara, B. K. Kumar, G. Srinivas, D. Ravinder, T. Vishnu, M. Sarasija, B. Sushmitha, *RSC Adv.* **2023**, *13*, 25–40.
[37] S. H. Olesen, J. Y. Zhu, M. P. Martin, E. Schonbrunn, *ChemMedChem* **2016**, *6*, 1137–44.
[38] B. J. Thompson, E. Sahai, *J. Cell Biol.* **2015**, *14*, 871–82.
[39] C.-Y. Cho, K.-T. Lee, W.-C. Chen, C.-Y. Wang, Y.-S. Chang, H.-L. Huang, H.-P. Hsu, M.-C. Yen, M.-Z. Lai, M.-D. Lai, *Oncotarget* **2016**, *7*, 14586–14604.
[40] V. Mallikanti, V. Thumma, K. C. Veeranki, S. Gali, J. Pochampally, *ChemistrySelect* **2022**, *7*, e202204020.
[41] V. Mallikanti, V. Thumma, R. Matta, K. R. Valluru, L. N. S. Konidena, L. S. Boddu, J. Pochampally, *Chemical Data Collections* **2023**, *45*, 101034.
[42] A. Daina, O. Michielin, V. Zoete, *Sci. Rep.* **2017**, *7*, 1–13.
[43] Y. C. Martin, *J. Med. Chem.* **2005**, *48*, 3164–3170.
[44] C. A. Lipinski, *Drug Discov Today Technol.* **2004**, *1*, 337–341.
[45] P. Ertl, A. Schuffenhauer, *J. Cheminf.* **2009**, *1*, 1–11.
[46] Y. Yutao, H. Fangjun, Z. Jingjing, X. Zhihui, C. Jianbin, Y. Caixia, T. Hongbo, L. Diansheng, J. Shuo, C. Fangqin, Y. Xuxiu, *Sens. Actuators B* **2012**, *166–167*, 665–670.
[47] X. Kangming, H. Fangjun, Z. Yongbin, W. Ying, C. Jianbin, Y. Caixia, *Sens. Actuators B* **2018** *255*, 2378–2383.
[48] K. Starzak, A. Matwijczuk, B. Creaven, A. Matwijczuk, S. Wybraniec, D. Karcz, *Int. J. Mol. Sci.* **2019**, *20*, 281.
[49] S. G. Pavel, A. T. Maxim, D. G. Yulia, I. L. Yana, V. E. Artur, E. T. Vladimir, F. A. Andrey, S. N. Mikhail, *Green Chem.* **2016**, *18*, 5984–5988.

[50] M. Kitamura, M. Yano, N. Tashiro, S. Miyagawa, M. Sando, T. Okauchi, *Eur. J. Org. Chem.* **2011**, 458–462.
[51] H. Cunjie, L. Jianping, Y. Liqiang, *Analytical Biochem.* **2019**, *566*, 32–36.
[52] Y. Sungho, E. A. Aaron, P. W. Audrey, J. C. Christopher, *J. Am. Chem. Soc.* **2005**, *127*, 16030–16031.
[53] K. Knepper, S. Vanderheiden, S. Brase, *Eur. J. Org. Chem.* **2006**, *2006*, 1886–1898.
[54] N. Perike, P. K. Edigi, G. Nirmala, V. Thumma, S. Bujji, P. S. Naikal, *ChemistrySelect* **2022**, *7*, e202203778.
[55] V. K. Chaitanya, P. Jalapathi, M. R. Chandar, T. Vishnu, M. Veerabhadraiah, M. Raghavender, *J. Iran. Chem. Soc.* **2023**, *20*, 995–1006.
[56] A. K. S. S. Madderla, R. Dharavath, N. Nalaparaju, R. Katta, S. Gundu, V. Thumma, P. B. D. Ashok, *J. Heterocycl. Chem.* **2022**, *59*, 1180–1190.
[57] S. H. Olesen, J.-Y. Zhu, M. P. Martin, E. Schonbrunn, *ChemMedChem* **2016**, *11*,1137–1144.

Manuscript received: February 23, 2023
Accepted manuscript online: May 19, 2023
Version of record online: June 12, 2023